Computed tomographic features of massive pneumoperitoneum in a dog with intestinal lymphoma – a case report

Sohee Lim[1,3], Yawon Hwang[1], Sangjune Sohn[1], Byunggyu Cheon[1], Chi Won Shin[2], Kichang Lee[3]

[1]Bupyeong SKY Animal Medical Center, Inchoen, Republic of Korea
[2]Seoul National University College of Veterinary Medicine, Department of Veterinary Clinical Sciences, Seoul, Republic of Korea
[3]Jeonbuk National University Specialized Campus, College of Veterinary Medicine, Iksan, Republic of Korea

Received June 15, 2021
Accepted May 4, 2023

Abstract

A 6-year-old intact male Jindo dog was presented for reduced appetite, depression, and tympanic abdominal distension. Abdominal radiographs showed severe pneumoperitoneum and an intestinal mass. Computed tomography revealed massive pneumoperitoneum associated with intestinal perforation, with cervical and thoracoabdominal wall emphysema, pneumomediastinum, pneumoretroperitoneum, pneumoscrotum, and peritonitis. Surgery confirmed a ruptured jejunal mass, and histopathologic evaluation of the excised tissues revealed intestinal lymphoma. Clinicians should therefore consider the possibility of gastrointestinal perforation in patients with severe pneumoperitoneum even where there is no history of trauma. Despite clinical stability, intensive monitoring and urgent decompressive intervention should be performed in patients with severe pneumoperitoneum.

Pneumoabdomen, emphysema, pneumoscrotum, gastrointestinal perforation

Pneumoperitoneum is an accumulation of gas within the peritoneal cavity, and was most often caused by gastrointestinal perforation resulting from neoplasia, steroids or nonsteroidal anti-inflammatory drugs (NSAIDs), abdominal surgery, or a ruptured urinary bladder. In human medicine, the speed and usefulness of computed tomography (CT) scans has made them an essential component of the pre-operative evaluation of patients with suspected gastrointestinal perforation (Borofsky et al. 2015). Computed tomographic features of massive pneumoperitoneum have been well-described in human medicine (Joo et al. 2020), but not in veterinary medicine.

Here, we describe the CT features of massive pneumoperitoneum with air distribution into numerous anatomic spaces in a dog with jejunal perforation.

Case history

A 6-year-old, 15.3 kg, intact male Jindo dog presented with a 5-day history of anorexia, depression, and abdominal distension. The dog had no history of trauma or previous illness and did not show any gastrointestinal symptoms such as vomiting or diarrhoea. Physical examination revealed tympanic abdominal distension with pain. The body temperature was 38.6 °C, the heart rate was 120 beats/min, and the respiratory rate was approximately 40 breaths/min. Complete blood count and serum biochemistry indicated leukocytosis (27.58×10^9/l reference interval: 6 to 17×10^9/l), granulocytosis (21.91×10^9/l reference interval: 3 to 12×10^9/l), and monocytosis (1.75×10^9/l reference interval: 0.2 to 1.5×10^9/l).

Right lateral and ventrodorsal radiographs of the thorax (49 kVp, 2.5 mAs) and abdomen (52 kVp, 2.5 mAs) were obtained (Vetter-DR9, Median International, Anyang, Korea).

Address for correspondence:
Kichang Lee
College of Veterinary Medicine
Chonbuk National University Specialized Campus
Iksan, Republic of Korea
E-mail: kclee@jbnu.ac.kr

Abdominal radiographs revealed a large amount of intra-abdominal gas and cranial displacement of the diaphragm, the surface of which was outlined by gas (Plate XI, Fig. 1). An oval-shaped gas filled mass (approximately 6.3 cm in diameter) was visible in the right dorsocaudal abdomen. Serosal detail, especially surrounding the mass, was lost, indicating abdominal effusion and peritonitis. Thoracic radiographs revealed no abnormalities aside from enlarged sternal lymph nodes. Abdominal ultrasonography was unsuccessful due to the large volume of air within the abdominal cavity and the pain experienced by the patient during palpation. The tentative diagnosis was gas leakage from a ruptured gastrointestinal tract.

Computed tomography scans were performed to identify the origin of the abdominal mass and to localize the suspected perforation. Images were obtained using a 32-slice helical CT scanner (Revolution ACT, GE Hangwei Medical Systems Co. LTd., Beijing, China, 120 kVp, 200 mA, 1.25 slice thickness) with the patient positioned in sternal recumbency. For contrast study, 600 mg iodine/kg of iopamidol (Pamiray 300 mgI/ml, Dongkook LifeScience, Seoul, Korea) was injected manually into the cephalic vein. Abdominal scans confirmed an extensive pneumoperitoneum collapsing the caudal vena cava (Plate XII, Fig. 2). The abdominal organs were ventro-centrally located and the diaphragm was cranially displaced by the intraperitoneal gas. Gas bubbles were found in the extraluminal spaces between the liver and intestinal segments. An ellipsoid mass (6.8 cm × 6.0 cm × 5.5 cm) with an irregular margin containing large amounts of air, fluid, and mineralized materials was found in the right caudal abdomen. Intact jejunal segments ran into and out of the mass. Except for the mass itself, the wall layering and degree of distension of the stomach and other parts of the intestines had no remarkable abnormalities. Hyperattenuated streaks, especially adjacent to the mass, were observed, indicating peritonitis or omentitis. Multiple abdominal lymph nodes were enlarged, and thoracic scans revealed a 1.5 mm pulmonary nodule and enlarged sternal lymph nodes. Gas bubbles were found in multiple extraluminal spaces, including the retroperitoneum, mediastinum, cervical and thoracoabdominal wall, pelvic cavity, and scrotal cavity (Plate XII, Fig. 3).

Laparotomy confirmed that the intestinal mass originated from the proximal jejunum. Omental redness and congestion as well as turbid peritoneal fluid containing intestinal contents were observed, suggesting septic peritonitis and omentitis (Plate XIII, Fig. 4). Other organs were grossly normal, with the exception of lymphadenomegaly, consistent with CT findings. The jejunal mass and inflamed omentum were removed, and intestinal anastomosis and peritoneal lavage were subsequently performed. The excised mass appeared dark red with irregular margins and distended with nodular and cystic structures. A small incision on the surface caused the gold-coloured intestinal contents to immediately burst out. Diffuse large cell lymphoma (high grade) was definitively diagnosed through histopathologic analysis. The pulmonary nodule was assumed to be pulmonary osteoma because of its small size and high attenuation. The probable cause of multiple lymphadenomegaly seemed to be reactive lymphadenopathy since the lymph nodes were mildly enlarged and the abdominal inflammation was severe. However, early and mild metastatic changes of some lymph nodes could not be ruled out because the additional cytohistologic evaluation of the enlarged lymph nodes had not been performed, and sternal lymph nodes gradually increased in size. Therefore, stage II or III would be presumed in applying the World Health Organization's clinical staging system for lymphoma (Withrow et al. 2013), even though the final tumour staging and classification was not achieved because the owner declined further diagnostic exploration after surgery.

After intensive postoperative care in five days, the patient was discharged without any complications, receiving supportive care without chemotherapy per the owner's request, and then was euthanized one month later due to gradual deterioration associated with presumed metastasis.

Discussion

Emergent and pre-operative CT evaluation in patients with suspected pneumoperitoneum due to gastrointestinal perforation is widely used in human medicine (Borofsky et al. 2015). Strong CT predictors of gastrointestinal perforations include extraluminal air bubbles, segmental bowel wall thickening, and focal wall defects (Hainaux et al. 2006). Other common findings are mesenteric fat stranding, bowel wall discontinuity, extraluminal fluid, abscess, and contrast extravasation (Hainaux et al. 2006; Borofsky et al. 2015; Pouli et al. 2020). In this case, the presence of extraluminal air adjacent to the intestines and in multiple other anatomic areas, focal wall thickening, perivisceral fat stranding, and extraluminal fluid were all features supportive of gastrointestinal perforation.

In cases of tension pneumoperitoneum, which is an extreme manifestation of pneumoperitoneum, patients may suffer from respiratory distress or hypothermia. In human medicine, tension pneumoperitoneum is a rare but life-threatening condition in which a large volume of air accumulates in the peritoneal cavity, causing a sudden increase in intra-abdominal pressure (Joo et al. 2020). The exit of air from the gastrointestinal lumen can lead to tension pneumoperitoneum because the surrounding omental fat prevents air from returning to the bowel, similar to a one-way valve mechanism (Joo et al. 2020). Computed tomographic features of tension pneumoperitoneum include elevation of the diaphragm, central displacement of the abdominal organs, and compression of the inferior vena cava, all of which can be attributed to increases in intra-abdominal pressure. These changes can lead to cardiorespiratory instability and, if severe enough, even result in cardiopulmonary arrest. Therefore, once this condition is recognized, urgent needle decompression or surgical intervention should be performed. In veterinary medicine, tension pneumoperitoneum has been reported in a cat with gastric perforation. The cat presented in shock with hypothermia, and abdominal radiographs suggested high intra-abdominal pressure due to severe pneumoperitoneum, similar to how pneumoperitoneum is described in human literature (Itoh et al. 2005). In the current case, abdominal CT scans revealed indicators of tension pneumoperitoneum common to humans, including cranial displacement of the diaphragm, ventrocentral displacement of the abdominal organs, and compression of the caudal vena cava. However, this patient did not show cardiorespiratory instability and was in a fairly stable condition. It is assumed that the haemodynamic state of the patient remained compensated despite a reduced preload. Nevertheless, if left untreated, this benign pneumoperitoneum could have developed into tension pneumoperitoneum. Therefore, prompt intervention and intensive monitoring were implemented.

In addition to the extensive pneumoperitoneum, our CT scans found mild pneumoretroperitoneum, pneumomediastinum, pneumoscrotum, and subcutaneous emphysema. While it is uncommon, subcutaneous emphysema following perforation of the gastrointestinal tract has been reported in humans (Whang et al. 1970; Joshi and Ganai 2015). Pneumoscrotum associated with gastrointestinal perforation has rarely been described in human medicine (Joshi and Ganai 2015). Notably, there have been no previous reports of subcutaneous emphysema and pneumoscrotum in dogs and cats with gastrointestinal perforation. One previous study hypothesized that air may spread to areas far from the site of perforation by moving along neurovascular bundles and fascial planes (Walker and Mozes 1981), while another has identified the possibility of air spread via direct gas diffusion or the perivascular sheath of the perforation (Whang et al. 1970). A recent review determined that ectopic gas can travel to numerous anatomical spaces, including the limbs, neck, mediastinum, retroperitoneum, peritoneum, extraperitoneum, and scrotum, via nerves and vascular sheaths, muscle intersections, and the fascia continuum (Vilaca et al. 2013). Aside from the intraperitoneal air, gas accumulated

in other extraluminal spaces was not clearly visible in the radiographs of this patient, nor has gas accumulation in these areas been described in previous veterinary reports. This could be attributed to the minute quantities of gas present or superimposition of the intraluminal gas.

In a previous veterinary report describing gastrointestinal ulceration in dogs, CT was found to be the most sensitive method (sensitivity of 93%) for identifying ulcers and perforation (Fitzgerald et al. 2017). Peritoneal fluid and gas bubbles were located within or near the gastrointestinal wall of the perforated ulcer. In addition, a recent report compared postmortem CT images with forensic autopsy findings in a dog with gastric ulceration and perforation caused by NSAID administration (Hamel et al. 2020). In both studies, CT images showed mild to moderate pneumoperitoneum in dogs with gastrointestinal perforation. However, to the best of our knowledge, CT features of massive pneumoperitoneum, with air distribution into numerous anatomic spaces, have not previously been reported in small animals.

In conclusion, this report described the CT features of a massive pneumoperitoneum with cervical, thoracic, and abdominal wall emphysema, pneumoretroperitoneum, pneumomediastinum, and pneumoscrotum in a dog with jejunal perforation due to neoplasia. Clinicians should consider the possibility of gastrointestinal perforation in patients with severe pneumoperitoneum even where there is no history of trauma. Computed tomography scans are rapid, provide information essential to identifying the underlying cause of the condition, and help physicians determine the proper treatment and surgical approach. Although significant cardiopulmonary instability was not observed in this patient, the CT features were very similar to those of tension pneumoperitoneum previously described in humans. Therefore, despite clinical stability, intensive monitoring and urgent decompressive intervention should be performed in patients with severe pneumoperitoneum.

References

Borofsky S, Taffel M, Khati N, Zeman R, Hill M 2015: The emergency room diagnosis of gastrointestinal tract perforation: the role of CT. Emerg Radiol **22**: 315-327

Fitzgerald E, Barfield D, Lee KCL, Lamb CR 2017: Clinical findings and results of diagnostic imaging in 82 dogs with gastrointestinal ulceration. J Small Anim Pract **58**: 211-218

Hainaux B, Agneessens E, Bertinotti R, De Maertelaer V, Rubesova E, Capelluto E, Moschopoulos C 2006: Accuracy of MDCT in predicting site of gastrointestinal tract perforation. Am J Roentgenol **187**: 1179-1183

Hamel PES, Stern AW, Grosso FV 2020: Gastric perforation in a dog: Postmortem computed tomography and forensic autopsy findings. Forensic Imaging **20**: 200359

Itoh T, Nibe K, Naganobu K, 2005: Tension pneumoperitoneum due to gastric perforation in a cat. J Vet Med Sci **67**: 617-619

Joo WJ, Kuwahara Y, Asaka Y, Mizu D, Hara S, Ariyoshi K 2020: Tension pneumoperitoneum caused by intestinal perforation from underlying colon cancer: a case report. J Med Case Rep **14**: 112

Joshi D, Ganai B 2015: Radiological features of tension pneumoperitoneum. BMJ Case Rep 21 June 2015

Pouli S, Kozana A, Papakitsou I, Daskalogiannaki M, Raissaki M 2020: Gastrointestinal perforation: clinical and MDCT clues for identification of aetiology. Insights Imaging **11**: 31

Vilaca AF, Reis AM, Vidal IM, 2013: The anatomical compartments and their connections as demonstrated by ectopic air. Insights Imaging **4**: 759-772

Walker MJ, Mozes MF 1981: Massive subcutaneous emphysema: an unusual presentation of jejunal perforation. Am Surg **47**: 45-48

Whang KC, Kim CS, Kim Y, Youn TY 1970: Subcutaneous emphysema due to perforation of the stomach. Yonsei Med J **11**: 203-207

Withrow SJ, Vail DM, Page RL 2013: Withrow & MacEven's Small Animal Clinical Oncology. Elsevier Saunders, Missouri, 612 p.

Fig. 1. Ventrodorsal (A) and right lateral (B) radiographs taken upon initial presentation. Note the marked pneumoperitoneum and an oval-shaped gas filled mass (arrow) at the dorsal abdomen. The cranial border of the diaphragm is outlined by free gas and is displaced cranially. Ventrodorsal (C) and right lateral (D) images were obtained three days after surgery. The severe pneumoperitoneum was resolved.

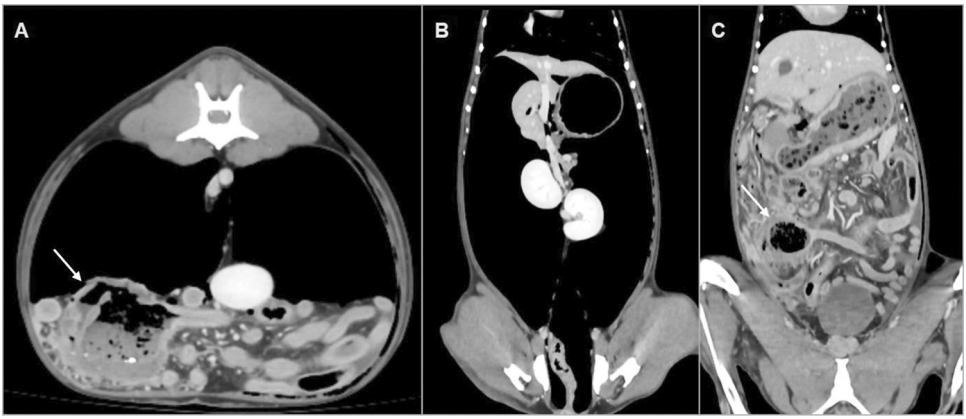

Fig. 2. Postcontrast transverse (A) and dorsal (B, C) CT images illustrating the severe pneumoperitoneum and air bubbles between the ventrally displaced intestines. An ellipsoid mass (arrow) originating from the jejunal segment with surrounding hyperdense streaky signs is shown.

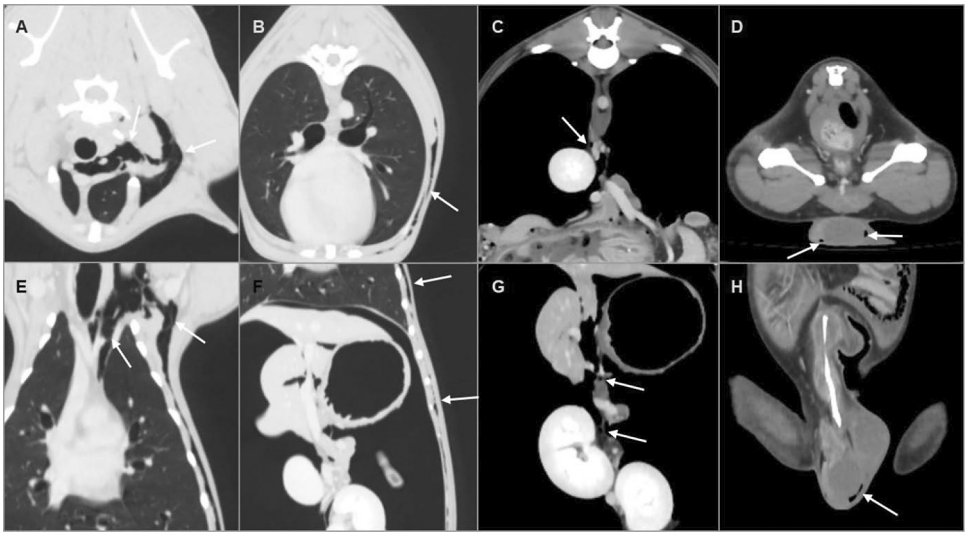

Fig. 3. Postcontrast transverse (A, B, C, D) and dorsal (E, F, G, H) CT images showing free air collection or bubbles (arrow) in the cranial mediastinum and neck (A, E), thoracic wall (B, F), retroperitoneum (C, G), and scrotal cavity (D, H). Note that the caudal vena cava appears elongated because of compression (C).

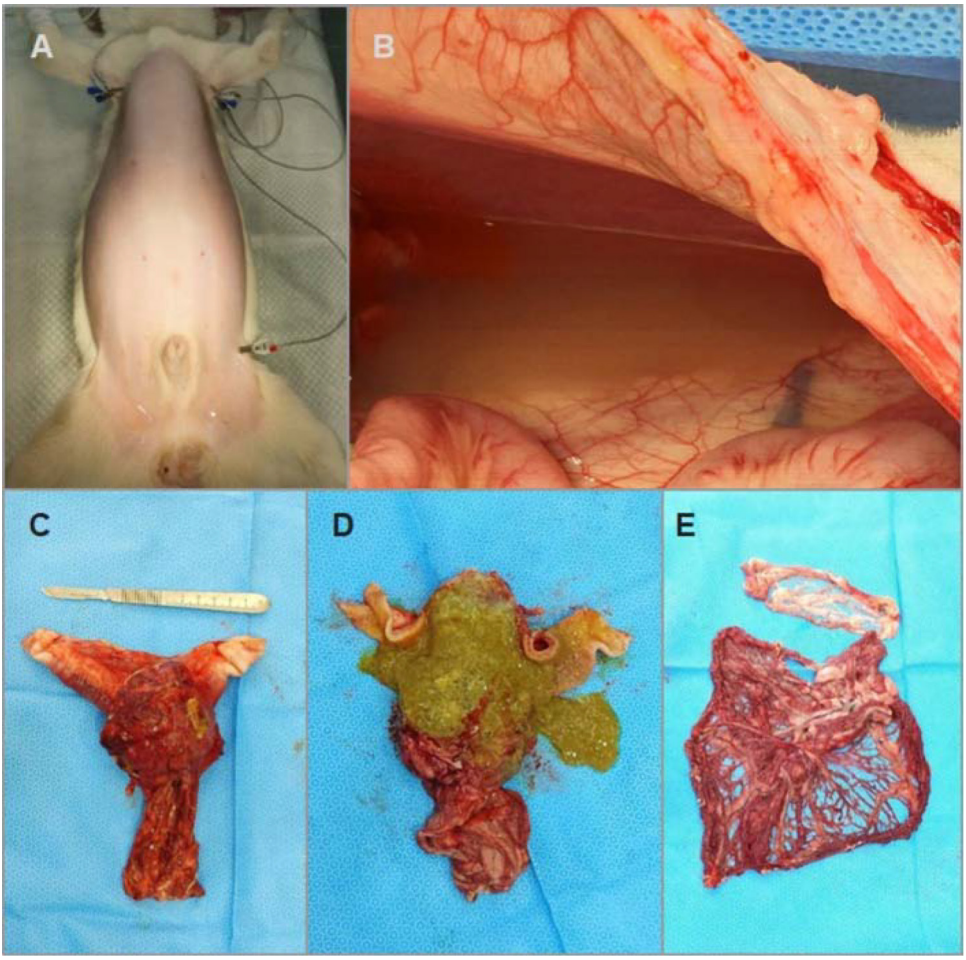

Fig. 4. Perioperative images showing marked abdominal distention (A), the turbid peritoneal fluid (B), the excised intestinal mass (C, D), and the omentum (E). The mass appears dark red and swollen with an irregular surface (C), and the intraluminal contents erupted with a small incision (D). The omentum appears dark red and congested.